Rakenteiden Mekaniikka (Journal of Structural Mechanics)
Vol. 47, No 2, 2014, pp. 67-79

On junction treatment in duct system flow analyses

Eero-Matti Salonen[1] and Rauno Holopainen

Summary. The article concerns the treatment of junctions when teaching duct system flows. In standard fluid mechanics textbook presentations only one static pressure value is usually associated with a junction. In engineering practice, however, pressure jumps over the junctions should be taken into account. The differences in the results by these two formulations are discussed in connection with three demonstration cases. The first case is treated initially with assumed constant friction factors so that closed form classroom hand calculations can be performed. More accurate numerical results are then obtained by a MATLAB program. The concept of a spurious dissipation is introduced to explain the apparently odd differences obtained by the two formulations.

Key words: duct flow, junctions, pressure jumps, spurious dissipation, CPF, DPF

Received 4 March 2014. Accepted 9 September 2014. Published online 31 October 2014.

Introduction

The article concerns the treatment of junctions when teaching duct system flows. In standard fluid mechanics textbook presentations only one static pressure value is usually associated with a junction, for example [1]. We will call this as *continuous pressure formulation* (CPF). In more specialized texts pressure jumps taking place at the junctions are taken into account, for example [2]. We will call this as *discontinuous pressure formulation* (DPF). The differences in the results obtained by these two formulations are discussed in connection with certain demonstration cases.

The governing equations in duct system flows are nonlinear and demand usually iterative solution approaches. Suitable simple enough hand calculation example cases are, however, needed for the students to assimilate the way the governing equations are generated. The example cases are taken this background in mind. For simplicity of presentation we do not take here into account gravity effects so the formulations apply more directly to air flows.

Three example cases are dealt with using in each both the DPF and CPF. Only in the first example case the hand calculation is performed in full detail in connection with the DPF. A constant friction factor value is used to simplify the treatment. All example cases are dealt with in addition by a MATLAB program taking into account in detail the effect of the friction factor. The results of the example cases reveal the unrealistic nature of the CPF — often employed in textbooks — for the treatment of duct system flows.

[1]Corresponding author. eero-matti.salonen@aalto.fi

First demonstration case

Duct data

Let us consider the duct system depicted in Figure 1. A symmetric simple demonstration example has been selected so that the governing equations can be generated and solved with relative ease using classroom hand calculations. In these we make a slight simplification. Additionally, some “exact” results without this simplification are given by two versions of a MATLAB program developed by the second writer [3]. We refer to these calculations and results by the attribute *Matlab* in the following. Hand calculations could be employed quite straightforwardly also in the second and third demonstration cases to follow. However, we will show in these cases only *Matlab* results as the purpose is just to detect some trends in the solutions when the relative duct section cross-sectional areas change.

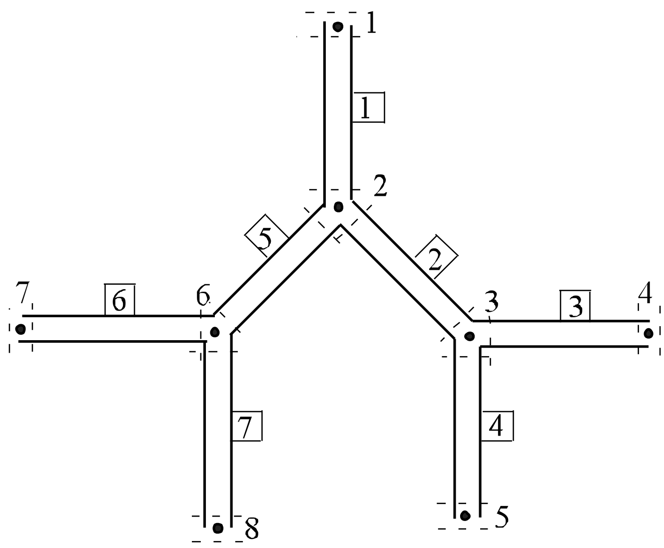

Figure 1. A duct system.

The channel sections have each the same length *L*, the same constant (circular) cross-sectional area *A* and the same roughness factor ε. The channel sections and the nodes (junctions) are numbered as shown in Figure 1. Node 1 is an inlet with an overpressure in the surroundings and nodes 4, 5, 7, 8 are outlets with zero pressure in the surroundings. From symmetry, we can restrict our hand calculations to the flow along channel sections 1, 2, 3 having nodes 1, 2, 3, 4.

We refer to the channel sections with superscripts in parentheses and to nodes by subscripts. To ease hand calculations we use the volumetric flow rate $Q^{(1)}$ in channel section 1 as a reference value and we denote it alternatively simply by *Q*. Similarly, assuming constant density fluid with density ρ, we employ the dynamic pressure in channel section 1 as a reference value and denote it by *P*:

$$P = \frac{1}{2}\rho\frac{Q^2}{A^2}. \tag{1}$$

The continuity equations at the junctions and symmetry give the flow rates

$$\begin{gathered} Q^{(1)} = Q, \\ Q^{(2)} = Q^{(5)} = Q/2, \\ Q^{(3)} = Q^{(4)} = Q^{(6)} = Q^{(7)} = Q/4. \end{gathered} \tag{2}$$

We assume in the standard way that the pressure drop or loss Δp in a channel section with a generic flow rate *q* can be expressed as

$$\Delta p = kq^2, \tag{3}$$

where the coefficient is given as

$$k = f\frac{L}{D}\frac{1}{2}\rho\frac{1}{A^2}. \tag{4}$$

Here *f* is the friction factor and *D* the hydraulic diameter of the duct. We assume in the hand calculations that *f* is a constant and thus also *k*. In the *Matlab* calculations the formula

$$f = \frac{0.25}{\left[\log\left(\frac{\varepsilon}{3.7D} + \frac{5.74}{\mathrm{Re}^{0.9}}\right)\right]^2} \tag{5}$$

is applied [4]. The Reynolds number

$$\mathrm{Re} = \frac{\rho D V}{\mu}, \tag{6}$$

where $V = q/A$ is the average velocity and μ is the viscosity of the fluid.

Discontinuous pressure formulation

As said, we will generate the equations needed to solve the flow rates and static pressures along the flow in channels 1, 2, 3 (and from symmetry then for the whole duct system) and include here the pressure jumps at the two junction nodes 2 and 3. The static pressures around nodes are denoted by symbols like $p_i^{(e)}$, where *e* refers to the channel section number and *i* to the node number.

The present discontinuous pressure approach introduces the student towards the actual real world treatment of junctions in engineering practice. However, we simplify here and assume that no losses (or more correctly said no dissipation) is taking place at the junctions.

First equation. Pressure loss equation at inlet node 1:

$$p_{\mathrm{s}} - \left[p_1^{(1)} + \frac{1}{2}\rho\frac{Q^2}{A^2} \right] = 0.5\frac{1}{2}\rho\frac{Q^2}{A^2}. \tag{7}$$

The loss coefficient has been taken as 0.5. Quantity p_{s} means the given static pressure in the surroundings. It is here driving the flow in the duct system. Using the reference pressure, the equation becomes

$$p_1^{(1)} = p_{\mathrm{s}} - \frac{3}{2}P. \tag{8}$$

Second equation. Pressure loss equation for channel section 1:

$$p_1^{(1)} - p_2^{(1)} = k\,Q^2. \tag{9}$$

Third equation. Pressure loss equation for channel section 2:

$$p_2^{(2)} - p_3^{(2)} = k\left(Q/2\right)^2. \tag{10}$$

Fourth equation. Pressure loss equation for channel section 3:

$$p_3^{(3)} - p_4^{(3)} = k\left(Q/4\right)^2. \tag{11}$$

Fifth equation. Pressure loss equation at outlet node 4:

$$\left[p_4^{(3)} + \frac{1}{2}\rho\frac{\left(Q/4\right)^2}{A^2} \right] - 0 = 1.0\frac{1}{2}\rho\frac{\left(Q/4\right)^2}{A^2}. \tag{12}$$

The loss coefficient has been taken to be 1.0 and the pressure in surroundings at zero. The equation gives simply the result

$$p_4^{(3)} = 0. \tag{13}$$

*Sixth equation***.** Pressure jump equation at junction 2:

$$\left[p_2^{(1)} + \frac{1}{2}\rho\frac{Q^2}{A^2} \right] - \left[p_2^{(2)} + \frac{1}{2}\rho\frac{\left(Q/2\right)^2}{A^2} \right] = C_2^{(1,2)}\frac{1}{2}\rho\frac{Q^2}{A^2}. \tag{14}$$

This is the way the total pressure jump is normally represented. $C_2^{(1,2)}$ is the junction coefficient for the total pressure jump from cross-section $2^{(1)}$ to cross-section $2^{(2)}$. The reference cross-section is $2^{(1)}$. As said, we work here assuming no losses at the junctions and we put thus $C_2^{(1,2)} = 0$. Using the reference pressure *P*, the equation becomes

$$p_2^{(1)} - p_2^{(2)} = -\frac{3}{4}P. \tag{15}$$

Seventh equation. Pressure jump equation at junction 3:

$$\left[p_3^{(2)}+\frac{1}{2}\rho\frac{(Q/2)^2}{A^2}\right]-\left[p_3^{(3)}+\frac{1}{2}\rho\frac{(Q/4)^2}{A^2}\right]=C_3^{(2,3)}\frac{1}{2}\rho\frac{(Q/2)^2}{A^2}. \qquad (16)$$

The meaning of the notations is obvious from the previous equation case. Putting $C_3^{(2,3)}=0$ gives

$$p_3^{(2)}-p_3^{(3)}=-\frac{3}{16}P. \qquad (17)$$

We have obtained seven equations corresponding to the seven unknowns Q, $p_1^{(1)}$, $p_2^{(1)}$, $p_2^{(2)}$, $p_3^{(2)}$, $p_3^{(3)}$, $p_4^{(3)}$. It is recalled that P is given by the definition (1).

Solution. Working backwards from node 4, we find

$$p_4^{(3)}=0, \qquad (18)$$

$$p_3^{(3)}=\frac{1}{16}kQ^2+p_4^{(3)}=\frac{1}{16}kQ^2+0=\frac{1}{16}kQ^2, \qquad (19)$$

$$p_3^{(2)}=p_3^{(3)}-\frac{3}{16}P=\frac{1}{16}kQ^2-\frac{3}{16}P, \qquad (20)$$

$$p_2^{(2)}=p_3^{(2)}+\frac{1}{4}kQ^2=\frac{1}{16}kQ^2-\frac{3}{16}P+\frac{1}{4}kQ^2=\frac{5}{16}kQ^2-\frac{3}{16}P, \qquad (21)$$

$$p_2^{(1)}=p_2^{(2)}-\frac{3}{4}P=\frac{5}{16}kQ^2-\frac{3}{16}P-\frac{3}{4}P=\frac{5}{16}kQ^2-\frac{15}{16}P, \qquad (22)$$

$$p_1^{(1)}=p_2^{(1)}+kQ^2=\frac{5}{16}kQ^2-\frac{15}{16}P+kQ^2=\frac{21}{16}kQ^2-\frac{15}{16}P. \qquad (23)$$

Equating (8) and (23) gives

$$p_s-\frac{3}{2}P=\frac{21}{16}kQ^2-\frac{15}{16}P \qquad (24)$$

or

$$p_s=\frac{21}{16}kQ^2+\frac{9}{16}P=\frac{21}{16}kQ^2+\frac{9}{16}\frac{1}{2}\rho\frac{Q^2}{A^2}=\left(\frac{21}{32}f\frac{L}{D}+\frac{9}{32}\right)\frac{\rho}{A^2}Q^2. \qquad (25)$$

Given the values of p_s, f, L, D, ρ, we can solve for Q. After that the pressures are obtained from (18) to (23).

As a detailed example case, we take the data

$$L=5\,\mathrm{m},\quad D=0.2\,\mathrm{m},\quad \rho=1.204\,\mathrm{kg/m^3}\quad p_s=100\,\mathrm{Pa}. \qquad (26)$$

The friction factor has been set to a fixed average value $f=0.02$ corresponding roughly to the velocities found. The solution is for the flow rate

$$Q = 0.367\,\text{m}^3/\text{s} \tag{27}$$

and for the static pressures

$$\begin{aligned} &p_1^{(1)} = -23.1\,\text{Pa}, \quad p_2^{(1)} = -64.1\,\text{Pa}, \quad p_2^{(2)} = -2.56\,\text{Pa}, \\ &p_3^{(2)} = -12.8\,\text{Pa}, \quad p_3^{(3)} = 2.56\,\text{Pa}, \quad p_4^{(3)} = 0. \end{aligned} \tag{28}$$

The *Matlab* calculations give with the values

$$\varepsilon = 0.9 \cdot 10^{-4}\,\text{m}, \quad \mu = 0.185 \cdot 10^{-4}\,\text{N s/m}^2, \tag{29}$$

the flow rate

$$Q = 0.368\,\text{m}^3/\text{s} \tag{30}$$

and the static pressures

$$\begin{aligned} &p_1^{(1)} = -23.9\,\text{Pa}, \quad p_2^{(1)} = -63.6\,\text{Pa}, \quad p_2^{(2)} = -1.61\,\text{Pa}, \\ &p_3^{(2)} = -12.4\,\text{Pa}, \quad p_3^{(3)} = 3.04\,\text{Pa}, \quad p_4^{(3)} = 0. \end{aligned} \tag{31}$$

The corresponding friction factor values are

$$f^{(1)} = 0.0192, \quad f^{(2)} = 0.0210, \quad f^{(3)} = 0.0236. \tag{32}$$

It is seen that the hand calculation and *Matlab* results are quite close to each other. The nearness of the guessed value $f = 0.02$ with those appearing in (32) explains this behavior.

Continuous pressure formulation

We repeat the calculations of the previous section now considering the static pressures on both sides of junctions 2 and 3 to be the same; that is, the static pressure distribution is assumed to be continuous. This is the way the pipe and channel systems are dealt with usually in elementary fluid mechanics textbooks. The sixth and seventh equations of the DPF are thus not needed here. We denote the static pressures at the nodes now only by the subscript referring to the node. Also $p_1 = p_1^{(1)}$ and $p_4 = p_4^{(3)}$. We write down the equations needed.

First equation. Pressure loss equation at inlet node 1:

$$p_1 = p_s - \frac{3}{2}P. \tag{33}$$

Second equation. Pressure loss equation for channel section 1:

$$p_1 - p_2 = k\,Q^2. \tag{34}$$

Third equation. Pressure loss equation for channel section 2:

$$p_2 - p_3 = k\left(Q/2\right)^2 . \tag{35}$$

Fourth equation. Pressure loss equation for channel section 3:

$$p_3 - p_4 = k\left(Q/4\right)^2 . \tag{36}$$

Fifth equation. Pressure loss equation at outlet node 4:

$$p_4 = 0 . \tag{37}$$

Working similarly as in the DPF case and using the same data, the hand calculation gives the flow rate

$$Q = 0.276\,\mathrm{m^3/s} \tag{38}$$

and the static pressures

$$p_1 = 30.4\,\mathrm{Pa}, \quad p_2 = 7.25\,\mathrm{Pa}, \quad p_3 = 1.45\,\mathrm{Pa}, \quad p_4 = 0 . \tag{39}$$

The *Matlab* results are

$$Q = 0.275\,\mathrm{m^3/s} \tag{40}$$

and

$$p_1 = 31.0\,\mathrm{Pa}, \quad p_2 = 8.12\,\mathrm{Pa}, \quad p_3 = 1.80\,\mathrm{Pa}, \quad p_4 = 0 . \tag{41}$$

The corresponding friction factor values are

$$f^{(1)} = 0.0199, \quad f^{(2)} = 0.0220, \quad f^{(3)} = 0.0250 . \tag{42}$$

Again, the hand calculation and *Matlab* results are close to each other.

There is a considerable difference between the flow rate obtained by the DPF and CPF; the latter gives here a smaller rate. In addition, the static pressure distributions are of totally different nature as can be detected from Figure 2. As no dissipation is taking place at the junctions, the DPF now gives correctly a continuous total pressure distribution. Of course, the junctions have in reality finite sizes and the relevant cross-sections situate at some distances from the nodes as is also obvious from Figure 1. This is ignored in Figure 2 so the pressure jumps seem to take place discontinuously.

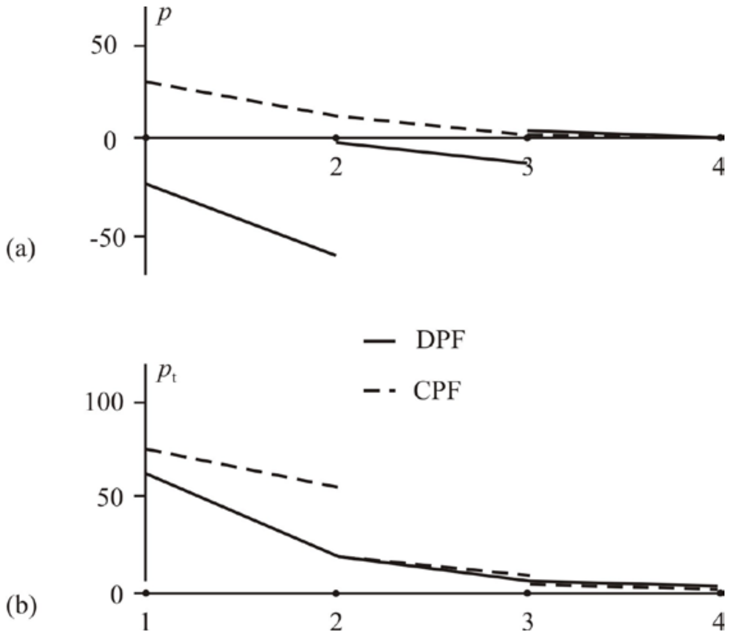

Figure 2. (a) Static pressure *p* [Pa] and (b) total pressure $p_t = p + \frac{1}{2} \cdot \rho V^2$ [Pa] distributions along channel sections 1, 2, 3 by the DPF and the CPF in the first demonstration case.

Second demonstration case

The duct system is taken to be otherwise the same as in the first case; only the diameters of the duct sections are changed to

$$\begin{aligned} D^{(1)} &= 0.2828\,\text{m}\,, \\ D^{(2)} = D^{(5)} &= 0.2\,\text{m}\,, \\ D^{(3)} = D^{(4)} = D^{(6)} = D^{(7)} &= 0.1414\,\text{m}\,. \end{aligned} \tag{43}$$

In fact, the ratios between the diameters of the consecutive channel sections have been selected to be $1/\sqrt{2}$ so that the ratios between the corresponding cross-sectional areas become $1/2$. The values used are taken on purpose so that the results by the DPF and CPF become identical. The reason for this behavior is explained later in the Explanation section.

The *Matlab* calculations give both in the DPF and CPF the same flow rate

$$Q = 0.458\,\text{m}^3/\text{s}\,. \tag{44}$$

The corresponding friction factor values are

$$f^{(1)} = 0.0188, \quad f^{(2)} = 0.0203, \quad f^{(3)} = 0.0221. \tag{45}$$

Further, the pressure jumps vanish in the DPF and the pressure distributions become identical. Without giving detailed numbers, the type of pressure distributions obtained are shown in Figure 3.

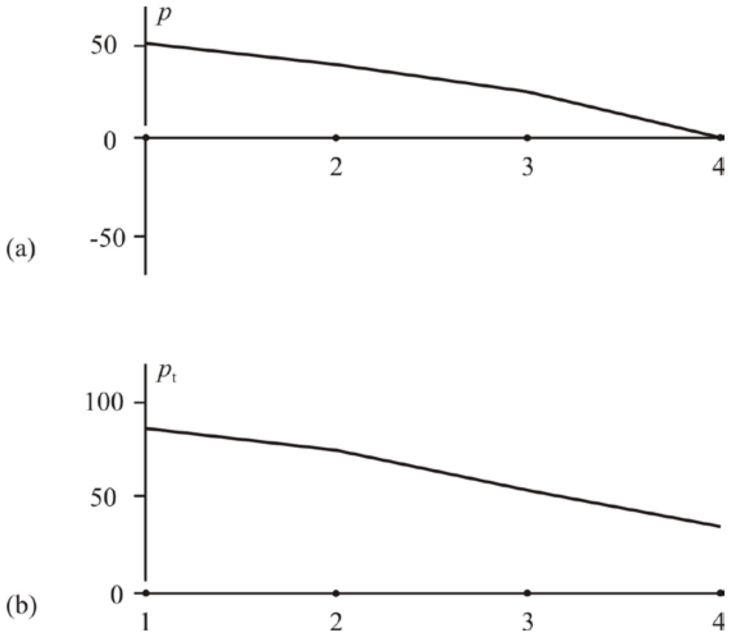

Figure 3. (a) Static pressure p [Pa] and (b) total pressure $p_{\mathrm{t}} = p + \frac{1}{2} \cdot \rho V^2$ [Pa] distributions along channel sections 1, 2, 3 by the DPF and the CPF in the second demonstration case.

Third demonstration case

Now the diameters of the duct sections are changed to

$$\begin{aligned} D^{(1)} &= 0.4\,\mathrm{m}\,, \\ D^{(2)} = D^{(5)} &= 0.2\,\mathrm{m}\,, \\ D^{(3)} = D^{(4)} = D^{(6)} = D^{(7)} &= 0.1\,\mathrm{m}\,. \end{aligned} \tag{46}$$

The ratios between the corresponding cross-sectional areas become $1/4$. The flow rate by *Matlab* is with the DPF

$$Q = 0.263\,\mathrm{m}^3/\mathrm{s} \tag{47}$$

and with the CPF

$$Q = 0.345\,\mathrm{m}^3/\mathrm{s}\ . \tag{48}$$

Contrary to the results in the first demonstration case, the CPF gives now the larger flow rate. The corresponding friction factor values are, respectively

$$f^{(1)} = 0.0213, \quad f^{(2)} = 0.0221, \quad f^{(3)} = 0.0236 \tag{49}$$

and

$$f^{(1)} = 0.0203, \quad f^{(2)} = 0.0212, \quad f^{(3)} = 0.0228\,. \tag{50}$$

The type of pressure distributions obtained are presented in Figure 4. Now the total pressure obtains positive jumps at junctions 2 and 3 with the CPF. This is unphysical and the behavior is explained in the next section.

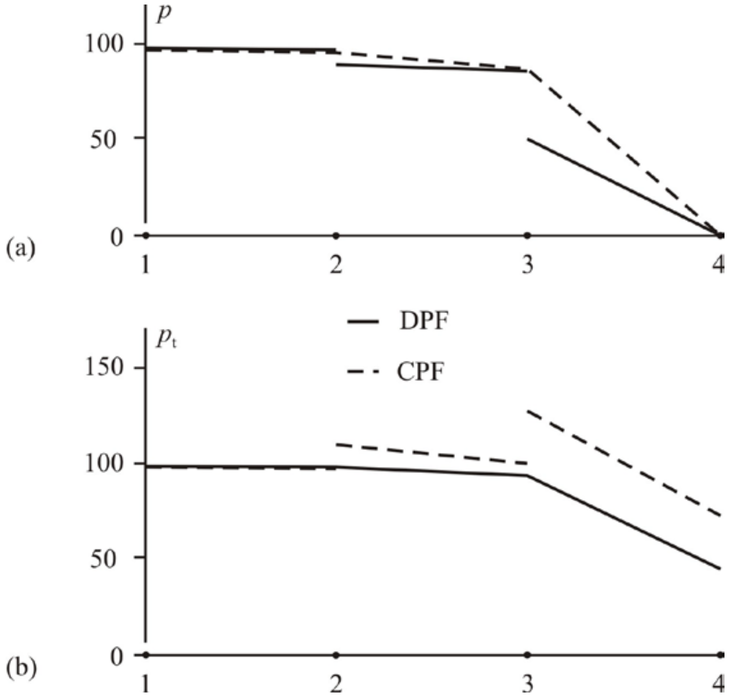

Figure 4. (a) Static pressure *p* [Pa] and (b) total pressure $p_t = p + \frac{1}{2} \cdot \rho V^2$ [Pa] distributions along channel sections 1, 2, 3 by the DPF and the CPF in the third demonstration case.

Explanation

The three example cases give results that may look at first sight somewhat confusing. The fluid mechanics course in which duct system flows are discussed has included probably also applications of the principle of the balance of mechanical energy in macroscopic form. This gives possibilities for clarifications.

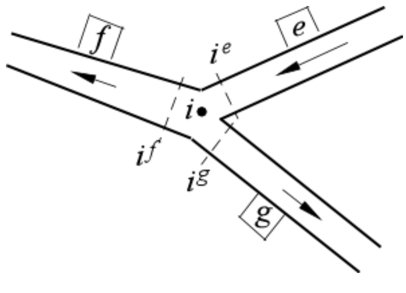

Figure 5. Generic notations for a diverging flow junction.

Let us consider a so-called diverging flow junction shown in Figure 5 and the control volume formed by the junction walls and by the three cross-sections $i^e \;\; i^f, i^g$. Making rather standard assumptions about the flow gives for the control volume the energy balance equation

$$\left[p_i^{(e)} + \frac{1}{2}\rho\frac{\left(Q^{(e)}\right)^2}{\left(A_i^{(e)}\right)^2}\right]Q^{(e)} - \left[p_i^{(f)} + \frac{1}{2}\rho\frac{\left(Q^{(f)}\right)^2}{\left(A_i^{(f)}\right)^2}\right]Q^{(f)}$$

$$-\left[p_i^{(g)} + \frac{1}{2}\rho\frac{\left(Q^{(g)}\right)^2}{\left(A_i^{(g)}\right)^2}\right]Q^{(g)} = D_i, \tag{51}$$

where D_i is the fluid dissipation rate in the control volume. We assume here that the three flows acting in the directions shown in Figure 5 are considered as positive.

It is not difficult to show that if the junction coefficients $C_i^{(e,f)}$ and $C_i^{(e,g)}$ are put to zero, the dissipation rate (51) vanishes. On the other hand, in the CPF we demand that

$$p_i^{(e)} = p_i^{(f)} = p_i^{(g)} \equiv p_i\,. \tag{52}$$

Using this and the junction continuity equation

$$Q^{(e)} - Q^{(f)} - Q^{(g)} = 0, \tag{53}$$

we find that the pressure cancels in (51) and we are left with

$$\left(D_{\mathrm{s}}\right)_i = \frac{1}{2}\rho\left[\frac{\left(Q^{(e)}\right)^3}{\left(A_i^{(e)}\right)^2} - \frac{\left(Q^{(f)}\right)^3}{\left(A_i^{(f)}\right)^2} - \frac{\left(Q^{(g)}\right)^3}{\left(A^{(g)}\right)^2}\right]. \tag{54}$$

We have denoted the dissipation rate now using the extra subscript s and we will call it as *spurious dissipation*. The explanation for this terminology is as follows. In real flows the fluid dissipation rate taking place at the junctions is for physical reasons always positive. However, with certain combinations of flow rates and cross-sectional areas (54) can become also negative. This means that energy is somehow supplied to the fluid from the junction!

The explanation here is that *the continuous pressure assumption is simply unrealistic* (inside the calculation model theory used in duct flows). In fact, we can imagine the continuous pressure setting to be achieved by introducing some devices such as small fans and valves inside the junction monitoring the flow in such a manner that the pressures at the inlet and at the two outlets become finally equal.

Let us consider now the demonstration cases and for example junction 2. Here we may put (see Figure 1) $e = 1$, $f = 2$, $g = 5$ in the generic formula (54):

$$(D_s)_2 = \frac{1}{2}\rho\left[\frac{Q^3}{\left(A^{(1)}\right)^2} - \frac{(Q/2)^3}{\left(A^{(2)}\right)^2} - \frac{(Q/2)^3}{\left(A^{(5)}\right)^2}\right] = \frac{1}{2}\rho\left[\frac{Q^3}{\left(A^{(1)}\right)^2} - 2\frac{(Q/2)^3}{\left(A^{(2)}\right)^2}\right]. \quad (55)$$

Symmetry in the flow rates and cross-sectional areas has been made use of.

Let us denote the cross-sectional area $A^{(2)}$ here simply as A. It is the same in all the demonstration cases. In the first demonstration example $A^{(1)} = A$ and the spurious dissipation

$$(D_s)_2 = \frac{1}{2}\rho\left[\frac{Q^3}{A^2} - 2\frac{(Q/2)^3}{A^2}\right] = \frac{1}{2}\rho\frac{3}{4}\frac{Q^3}{A^2} \quad (56)$$

is positive.

In the second demonstration case $A^{(1)} = 2A$ and the spurious dissipation

$$(D_s)_2 = \frac{1}{2}\rho\left[\frac{Q^3}{(2A)^2} - 2\frac{(Q/2)^3}{A^2}\right] = 0\,. \quad (57)$$

In the third demonstration case $A^{(1)} = 4A$ and the spurious dissipation

$$(D_s)_2 = \frac{1}{2}\rho\left[\frac{Q^3}{(4A)^2} - 2\frac{(Q/2)^3}{A^2}\right] = -\frac{1}{2}\rho\frac{3}{16}\frac{Q^3}{A^2} \quad (58)$$

is negative.

Similar expressions can be found at junction 3 and 6. Now the nature of the results produced by the CPF can be understood. In the first case positive spurious dissipation is generated slowing the flow. In the second case no spurious dissipation appears and the two formulations give identical results. In the third case negative dissipation (or positive energy input) is generated speeding the flow.

Concluding remarks

The spurious dissipation concept can be introduced equally well for a converging flow junction to explain seemingly odd results by the two formulations. The concept can be extended also for water flow, where the gravity effects must be accounted for. Finally, as is well known, and should be stressed to the students, the calculation models for duct and pipe flows contain certain assumptions not in accordance with reality. One of these is to assume that the losses to take place in a pointwise way at valves and at junctions. In reality, the losses occur along the ducts and mainly in the downwind parts. However, when applying these calculation models, we can also assume the spurious dissipation to act in a pointwise way. Additional comments concerning junction modeling can be found in [5].

Acknowledgements

We want to thank the reviewers for pointing out certain errors in the original manuscript and for suggestions for improvements.

References

[1] F. M. White, *Fluid Mechanics*, 2nd ed., McGraw-Hill, 1987.
[2] *ASHRAE Handbook, Fundamentals*, Chapter 32, Duct Design, 1997.
[3] E.-M. Salonen and R. Holopainen, A PQ-Formulation for Ventilation Duct System Flow Analyses, *International Journal of Ventilation*, **7**, (5), 2008, pp. 251-265.
[4] P. K. Swamee and A. K. Jain, Explicit Equations for Pipe-Flow Problems, *Journal of Hydraulics Division*, ASCE, Vol. 102, No. HY5, May, 1976, pp. 657-664.
[5] E.-M. Salonen and R. Holopainen, Notes on Junction Coefficients, *International Journal of Ventilation*, **9**, (2), 2010, pp. 191-196.

Eero-Matti Salonen
Aalto University, Department of Civil and Structural Engineering
P.O.Box 12100, FI -00076, Finland
eero-matti.salonen@aalto.fi

Rauno Holopainen
Finnish Institute of Occupational Health
Work Environment Development
Arinatie 3A, FI-00370, Finland
rauno.holopainen@ttl.fi